Aalborg Universitet

AALBORG UNIVERSITY

Distributed Bus Signaling Control for a DC Charging Station with Multi Paralleled Flywheel Energy Storage System

Sun, Bo; Dragicevic, Tomislav; Vasquez, Juan Carlos; Guerrero, Josep M.; Savaghebi, Mehdi

Distributed Bus Signaling Control for a DC Charging Station with Multi Paralleled Flywheel Energy Storage System

Bo Sun, Tomislav Dragicevic, Juan C. Vasquez, Josep M.Guerrero, Mehdi Savaghebi
Department of Energy Technology – Microgrid Research Programme www.microgrids.et.aau.dk
Aalborg University, Denmark

Abstract— **Fast charging stations (FCS) will become an essential part of future transportation systems with an increasing number of electrical vehicles. However, since these FCS plugs have power ratings of up to 100 kW, serious stress caused by large number of FCS could threaten the stability of the main power grid. To overcome the possible adverse impacts, this paper applies a dedicated paralleled flywheels energy storage system (ESS) in FCS, to balance the power by the method of ramping the initial power peak. Distributed DC-bus signaling (DBS) method is employed in the power coordination of grid and flywheel converters, and the two flywheels are able to share the power peak through the voltage vs speed droop control. Furthermore, a reduced small-signal model has been built for the purpose of stability analysis and parameter optimization. Finally, real-time simulation results performed on a reduced scale model corresponding to experimental setup parameters have been reported in order to verify the validity of proposed approach.**

Keywords—EV charging; flywheel energy storage system; distributed bus signaling

I. INTRODUCTION

Due to the increasing conventional fossil fuels' consumption and serious environmental pollution caused by carbon dioxide emissions, the electric vehicles (EV) have a great potential to be the dominate transportation choice in near future [1-2]. Plug-in hybrid electrical vehicle (PHEV) is currently a much more cost-effective choice for customers, expected to replace the traditional vehicles and have a considerable numbers of users in the future. Therefore, providing an acceptable surroundings and necessary ancillary services of PHEV fleets is a critical issue of next generation smart grid.

Up to now, the power rating of FCS could be up to 100 kW [3], so the impact of a large number of PHEV chargers integration to network should be seriously concerned. The sudden connection of EV chargers could cause a high power shock to the grid, and lead to rising of peak loading of distributed system that may cause the instability of the distributed network.

In order to cope with issues above mentioned, several methods have been proposed. In [4], [5], a vehicle to grid (V2G) concept has been proposed to utilize the energy stored in batteries of all the EV connected to the grid to alleviate the adverse state in grid and maintain the safe operation of network. However, this way may threaten the standard battery charging algorithms and harm the lifetime of EV battery. In [6], a dedicated battery energy storage system (BESS) is connected to a common DC bus to supply part of charging power. However, direct connection of battery pack may cause the unregulated DC voltage deviations and frequent charging cycling and high peak current caused by PHEV charger connection would accelerate the degradation of battery. Compared to BESS, flywheel energy storage system (FESS) could compensate the peak power with a faster response and support a larger numbers of charge/discharge cycles. In past, FESS has been extensively used for DC-link coupled power balancing in grid-connected applications [7] [8]. However, in all of past applications, the system employed a centralized supervisory controller through the communication between flywheel controller and grid controllers. In [9], a distributed DC-bus signaling (DBS) strategy is applied for FCS control with a flywheel ESS to realize the distributed coordination of each unit in system. However, only one flywheel ESS is considered in [9]. Regarding the SOC balance control, in [10] [11], the system with multi BESS system is analyzed based on the SOC adaptive droop control to realize the power and current sharing of each battery ESS. And in [12][13], a fuzzy control method and adaptive droop are used respectively deployed to balance the control of energy storage system, however, most previous control scheme is discussed based on BESS.

In this paper, a multi paralleled flywheels based ESS driven by induction machine (IM) is employed and DBS strategy is applied for the purpose of internal power coordination between units, and speed vs DC voltage droop control is used for paralleled flywheels control. The proposed scheme could realize the internal power balancing against the negative effect caused by HEV sudden connection, and be expanded to seamlessly connect more flywheels ESS. The rest of the paper is organized as follows: Section II presents the structure of the charging station upgraded with multi flywheel energy storage system and analyzes the characters of each part of the CS. In Section III, a supervisory control is demonstrated based on DBS strategy to realize the coordinate control of grid converter and flywheel converters. Section IV, a small-signal stability model is analyzed based on the CS system with two flywheels. Section V shows the real-time simulation results based on dSPACE1006. Finally, Section VI gives the conclusion.
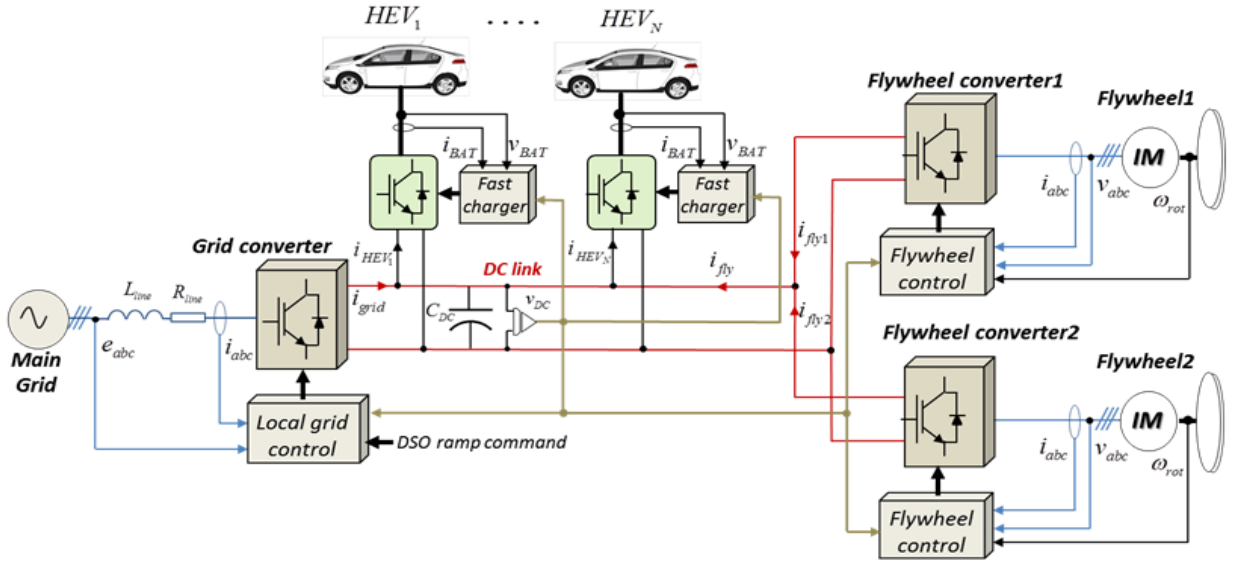
Fig. 1. Structure of the FCS system

II. STRUCTURE OF CHARGING STATION

First, Fig.1 depicts the basic structure of FCS system upgraded with two dedicated FESS, including a set of DC/DC converters serving as HEV chargers and a number three-phase AC/DC converters connected with grid and paralleled flywheels, respectively. All the power electronics interfaces are connected to a common DC bus. According to Kirchhoff's law, the system dynamic current around DC-link capacitor could be derived as follows:

$$C_{DC}\frac{dv_{DC}}{dt} = i_{grid} + i_{fly} - i_{HEV} \tag{1}$$

Where C_{DC} is the capacitance connected to the bus, i_{grid} and i_{fly} are the DC currents flowing from the grid and flywheel, respectively, while i_{HEV} is the current extracted by the fast DC charger(s). The HEV charger, grid interface and flywheel have their own specific dynamic features, so it is necessary to study the effect produced by each unit, in order to obtain the stability properties of the whole system.

(1). HEV charger. A buck DC/DC converter is applied as EV charger following the control scheme provided by battery manufacturer which includes constant current and constant voltage charging stages. Since current and voltage only have relationship with battery, this system does not need any feedback signals from FCS. Additionally, a low bandwidth controller is commonly derived since it is not critical to control with a rapid response for EV charging process. Taking into account all above, the current introduced by the HEV charger may be regarded as a disturbance input that does not affect the system dynamic properties.

2). Grid interface. A two-level PWM rectifier is used to connect grid, and the control scheme is deployed in stationary ($\alpha - \beta$) reference frame, the DC voltage controller and reactive power controller that is zero in this paper generate the Id and Iq reference, then Idref and Iqref are transferred to

stationary frame as I_{α_ref} and I_{β_ref} . The current controller in stationary frame employs the PR controller, which could obtain the same response as the PI controller in d-q frame to track the reference generated by voltage controller [14]. On the other hand, in this paper, as the stability analysis is derived based on DC-link and only active power exchange is considered in this application, the analysis in synchronous (d-q) frame is easier to obtain the control block. In synchronous frame, it could be obtained that:

$$\begin{bmatrix} \dot{i}_d \\ \dot{i}_q \end{bmatrix} = \frac{v_{DC}}{L_{line}}\begin{bmatrix} d_d \\ d_q \end{bmatrix} + \begin{bmatrix} -\dfrac{R_{line}}{L_{line}} & \omega \\ -\omega & -\dfrac{R_{line}}{L_{line}} \end{bmatrix}\begin{bmatrix} i_d \\ i_q \end{bmatrix} - \frac{1}{L_{line}}\begin{bmatrix} e_d \\ e_q \end{bmatrix} \tag{2}$$

where i_q and i_d , d_q and d_d are DC-like currents and duty ratios aligned with q and d rotating axes, respectively, while R_{line} and L_{line} are per phase resistance and inductance of the AC line.

It is assumed that the I_d and I_q reference are followed instantaneously, and considering the grid voltage is synchronized with d-axis and reference for q axis is set to zero, the DC link current from grid could be expressed as:

$$i_{grid} = 1.5\frac{v_d i_d}{v_{DC}} \tag{3}$$

(3) may be linearized around the operating DC voltage, obtaining:

$$\hat{i}_{grid} = 1.5\frac{(e_d + 2I_d R_{line} + I_d L_{line}s)}{V_{DC}}\hat{i}_d \tag{4}$$
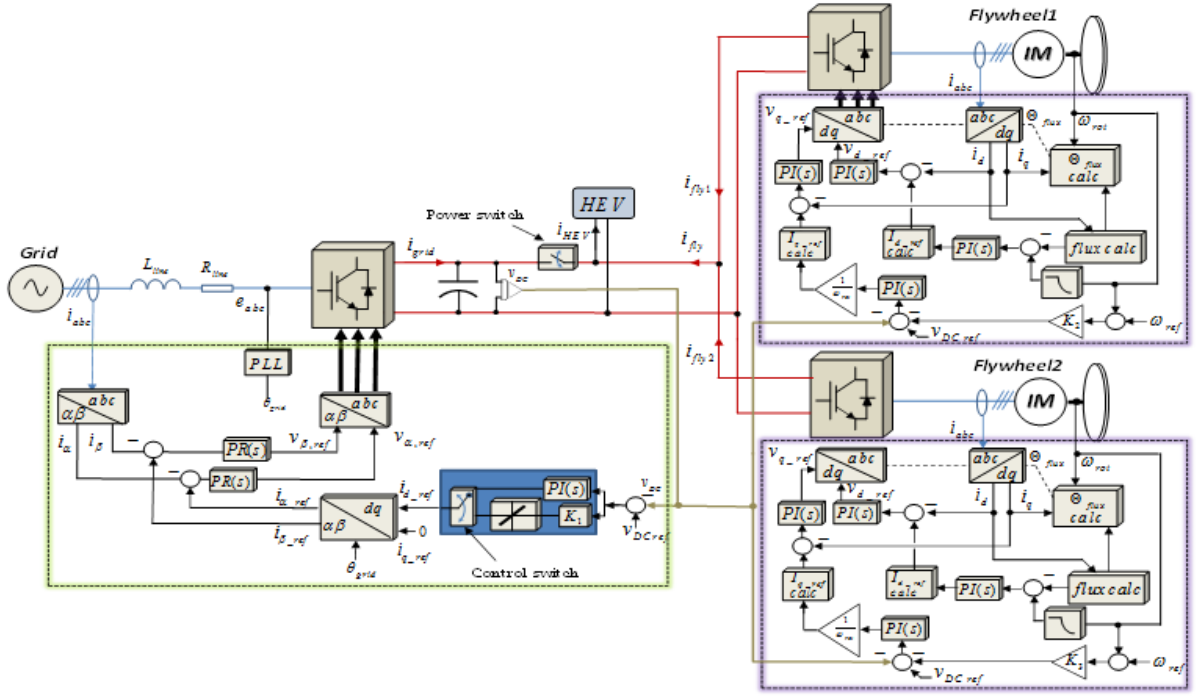
I_d is the equilibrium value of i_d .

Fig. 2. Flywheel and grid converter control scheme

(3). Flywheel energy storage system: In this paper, two paralleled flywheels based on induction machine are employed, and the parameters and control of two flywheels are the same. The inner control scheme for IM adopts the indirect field oriented control which is considered to have a fast and accurate response. The synchronous reference frame is also used for modeling and control of the machine, where d-axis component corresponds to flux and q axis component corresponds to torque. Based on this classical vector control approach, the d-q model in flux coordinates can be represented as follows:

$$\begin{bmatrix} \overset{\cdot}{i_d} \\ \overset{\cdot}{i_q} \end{bmatrix} = \frac{v_{DC}}{\sigma L_s}\begin{bmatrix} d_d \\ d_q \end{bmatrix} + \begin{bmatrix} -\dfrac{R_s}{\sigma L_s} & \omega_{mR} \\ -\omega_{mR} & -\dfrac{R_s}{\sigma L_s} \end{bmatrix}\begin{bmatrix} i_d \\ i_q \end{bmatrix} - \frac{1}{\sigma L_s}\begin{bmatrix} 0 \\ \omega_{mR}\psi_r\dfrac{L_0}{L_r} \end{bmatrix} \quad (5)$$

where L_s, L_r, R_s, R_r are stator and rotor inductances and resistances, respectively and L_0 is the mutual inductance; i_d and i_q are d and q-axis currents in field coordinates, ω_{mR} is the flux rotational speed, i_{mR} is the magnetizing current, while ψ_r is the rotor flux; σ is the total leakage coefficient.

The flywheel current flowing towards the common DC bus may be expressed as:

$$i_{grid} = 1.5\frac{v_d i_d + v_q i_q}{v_{DC}} \quad (6)$$

The resulting expression around V_{DC} could be linearized as:

$$\hat{i}_{fly} = 1.5\frac{2(R_s + \left(\dfrac{L_0}{L_r}\right)^2 R_r)I_q + \dfrac{\omega_{rot0}L_0^2 I_d}{L_r} + \sigma L_s I_q s}{V_{DC}}\hat{i}_q \quad (7)$$

The swing equation of the flywheel governs the changes in the rotational speed of the rotor:

$$J\frac{d\omega_{rot}}{dt} = 1.5p(1-\sigma)L_s i_{mR} i_q \quad (8)$$

Where J is the flywheel inertia and p is the number of pole pairs.

III. SUPERVISORY CONTROL SCHEME

The complete control diagram of the system is depicted in Fig.2. The task of the FCS supervisory control is to realize balanced power coordination between the grid-connected rectifier and flywheels at the moment of HEV chargers sudden connection to common DC bus. Its main purpose is to alleviate the adverse impact of a sudden current step caused by HEV charger by utilizing energy stored in flywheel.

According to variations of the common DC voltage driven by a sudden connection of HEV charger, the currents given by GC and FC are regulated in a distributed manner. In order to implement three voltage controllers that operate in parallel, a Speed vs. DC voltage droop has been installed on top of FC voltage controller, since energy stored in flywheel is a function of its rotational speed. On the other hand, the voltage controller of GC uses a rate limiter to limit the current flowing from the grid in a low ramp.

$$\left(-F_1K_2k_{pq1}-F_2K_3k_{pq2}C_{DC}+g_{1p}K_1+k_{pq1}g_{2p}+k_{pq2}g_{3p}\right)s^4+\left(\begin{array}{c}-F_2K_3k_{pq2}C_{DC}-F_1K_2k_{iq1}C_{DC}-F_2K_3k_{iq2}C_{DC}-F_1F_2K_2K_3k_{pq1}k_{pq2}g_{1p}-F_2K_1K_3k_{pq2}g_{1p}\\ +k_{iq1}g_{2p}+k_{iq2}g_{3p}\end{array}\right)s^3$$

$$+\left(\begin{array}{c}F_1F_2K_2K_3k_{pq1}k_{iq2}C_{DC}+F_1F_2K_2K_3k_{pq2}k_{iq1}C_{DC}-F_1K_1K_2k_{iq1}g_{1p}-F_2K_1K_3k_{iq2}g_{1p}+F_1F_2K_1K_2K_3k_{pq1}k_{pq2}g_{1p}-F_2F_3k_{pq1}k_{iq2}g_{2p}-F_2K_3k_{pq2}k_{iq1}g_{2p}\\ -F_1K_2k_{pq2}k_{iq1}g_{3p}-F_1K_2k_{pq1}k_{iq2}g_{3p}\end{array}\right)s^2 \quad (9)$$

$$+\left(F_1F_2K_1K_2K_3k_{iq1}k_{iq2}C_{DC}+F_1F_2K_1K_2K_3k_{pq1}k_{iq2}g_{1p}+F_1F_2K_1K_2K_3k_{pq2}k_{iq1}g_{1p}-F_2F_3k_{iq1}k_{iq2}g_{2p}-F_1K_2k_{pq1}k_{pq2}g_{3p}\right)s+F_1F_2K_1K_2K_3k_{pq1}k_{iq2}g_{1p}=0$$

According to the hierarchical control scheme, the process of the coordination dealing with the sudden connection of HEV could be as follows:

1). the sudden connection of HEV charger leads to the DC voltage drop, the rate limiter in grid controller will get saturated;

2). flywheel will supply all the active power required by charger by reducing its rotational speed;

3). DC bus recover to a value according to the speed vs DC voltage droop, meanwhile the grid current increase specified by the rate limiter.

4). from the point that the grid current is equal to the HEV current, the grid current supply all the power to HEV and starts to recharge the flywheel to the nominal speed.

IV. STABILITY ANALYSIS

Combining the models of GC and FC presented in (4) and (7) with the loops, belonging to upper control layer (see Fig. 2), the block diagram of control could be obtained in Fig. 3. In the control block, G1 is obtained from (4) and can be simplified as $G_1 = g_{1p} + s \cdot g_{1d}$, G2 and G3 are derived from (7) and can be simplified as $G_2 = g_{2p} + s \cdot g_{2d}$ and $G_3 = g_{3p} + s \cdot g_{3d}$, F is the swing equation in (8).

Taking into account complete representations of all transfer functions in the model and neglecting some terms that are several orders of magnitude lower than other, a fourth order characteristic equation may be derived as shown in (9) on the top of this page.

The most influential parameter on response is K1 (gain of GC), K2 and K3 (droop coefficient of flywheel 1 and 2), As flywheel 1 and flywheel 2 have the same parameter, K2 and K3 could be set to the same value, a family of root locus for different K2 (K3) could be plotted in fig. 4 for changing K1 from 0.5 to 10. As a trade-off, K1=1.25, K2=K3=0.2 are chosen.

TABLE I. REAL-TIME SIMULATION PARAMETERS

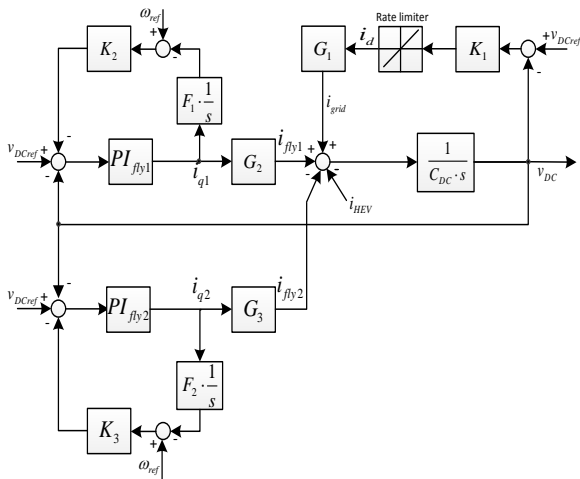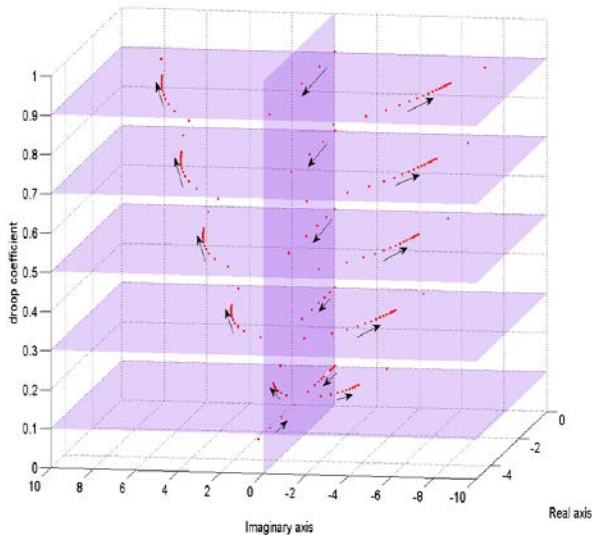| Electrical parameters	
C_{DC}	2.2mF
L_{line}	3.8mH
R_{line}	0.2Ω
$V_{grid}(p-p)$	325V
Induction machine parameters	
L_s	0.01160494 mH
L_r	0.01160494 mH
σ	0.5556
J	0.8 kgm^2
R_s	1.945 Ω
R_r	2.3736 Ω
T_{fly}	1e-4s
GC controller	
K_1	1.25
i_{rate}	0.5 A / s
T_{grid}	1e-4s
FC controller	
ω_{ref}	157 rad/s
K_2	0.2
K_3	0.2

Fig. 3. Control block of system

Fig. 4.Family of root locus for changing K1,K2 and K3 of the system

V. REAL-TIME SIMULATION

A reduced scale model corresponding to the experimental setup parameters of the plant, as presented in Fig. 2 was assembled in Matlab/Simulink and compiled into dSPACE 1006. The parameters used for simulation may be found in Table I.

Simulation of the moment of connection of HEV to the charging station has been performed for two cases. The first one is conventional scheme without dedicated FESS. The second is the proposed scheme with two paralleled flywheels ESS.

Simulation was performed for one full discharge/charge cycle of the flywheel ESS following the connection of HEV(s) at 11 seconds. Waveforms of respective DC currents and DC voltage for both cases are shown in the same figures in order to clearly demonstrate the differences in their performances. Fig. 5(a) shows the DC bus voltage and from HEV connection to charging completed and the zoomed-in waveforms of starting of HEV connection are shown in Fig. 6(b).

Fig. 6 shows the DC current of grid converter, HEV and flywheel respectively, it can be seen that the flywheel first supply the sudden power request from HEV charger, the grid current increases gradually according to a slow rate, when it equalizes the HEV current at around 15s, the grid converter takes charge of the HEV charging and starts to charge the flywheel.
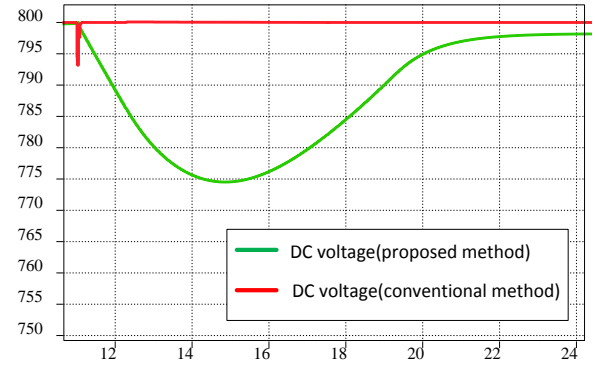
(a)
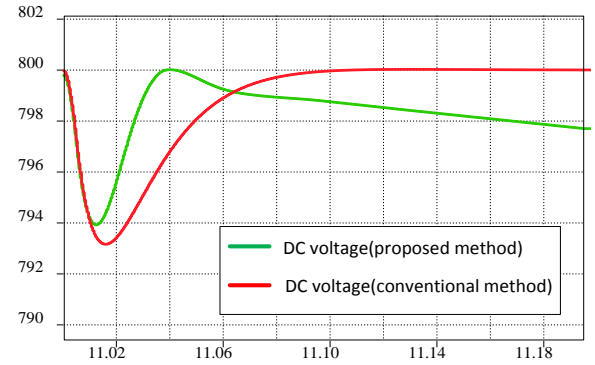
(b)

Fig. 5.DC Bus voltage. (a) DC bus voltage (b) zoomed-in DC bus voltage

The waveforms of the current and speed of two flywheels are presented in Fig. 7 and Fig. 8. It is observed that the flywheels are able to share the DC load current according to the speed vs DC voltage droop control scheme. When the EV connected at 11s, the flywheel speed reduced according to the droop law, meanwhile the power flows back to the DC bus to supply the energy for the load.

The Fig.9 shows the grid converter AC-side current in proposed and conventional schemes respectively. As it is observed, in the proposed scheme the grid-side current increase with a ramping that means that the sudden connection of EV does not cause an impact to grid, while in conventional scheme the grid converter current increase in a step manner, so that it may lead to a shock to the grid if a large amount of high-power EVs are connected to the station.
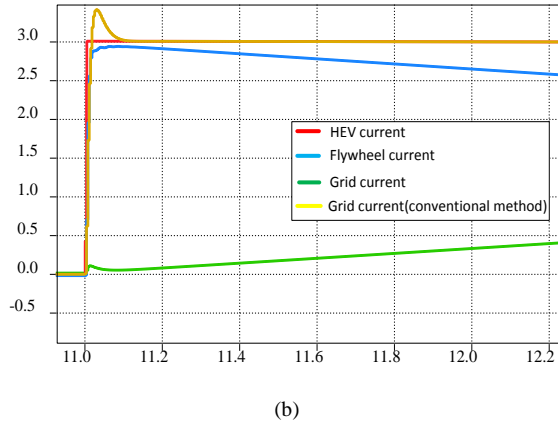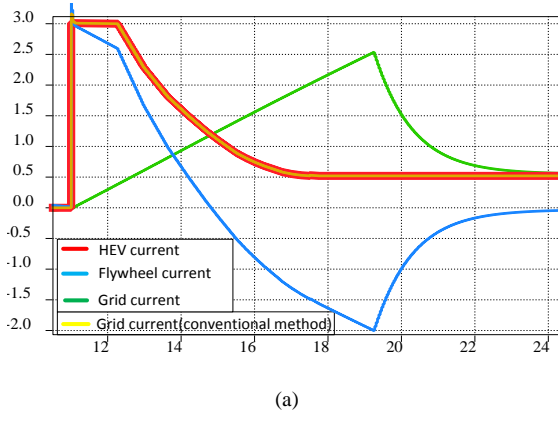
(a)

(b)

Fig. 6. DC current (a) DC currents of Flywheel, grid converter and HEV (b) Zoomed-inDC currents of Flywheel, grid converter and HEV
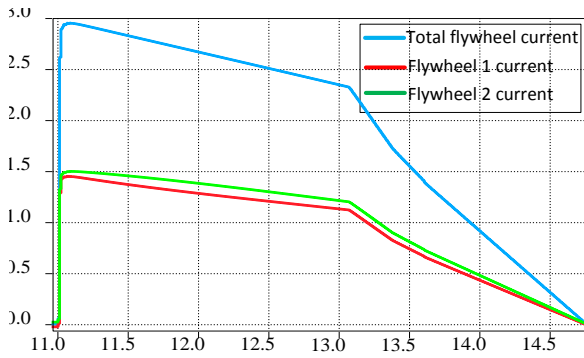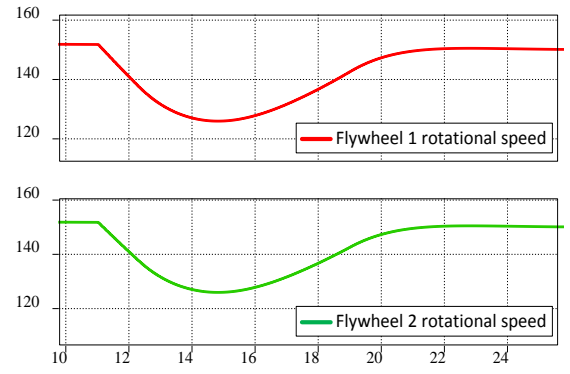

Fig. 7. DC current of two flywheels

Fig. 8.   Flywheels speed
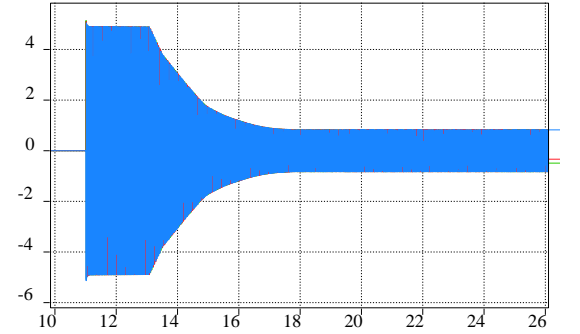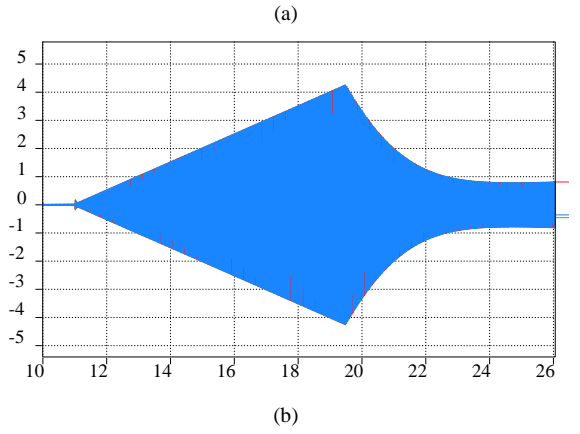

(a)

(b)

Fig. 9. Grid converter AC current (a) proposed scheme (b) conventional scheme

VI. Conclusions

This paper employs a dedicated paralleled flywheels ESS in a fast charging station. The proposed scheme uses distributed DC bus signals for power coordination of each unit and DC voltage vs speed droop control for paralleled flywheels. A reduced order small signal stability model was analyzed to study the stability and parameter optimization. The proposed strategy could compensate the initial power peak by sudden HEV connection and limit the rate of grid current increase in a distributed manner. The real-time simulation results validate the feasibility of proposed scheme.

REFERENCES

[1] A. Emadi, M. Ehsani, and J. Miller, Vehicular Electric Power Systems: Land, Sea, Air, and Space Vehicles. The Power engineering, Taylor & Francis, 2010.

[2] X. Chang, B. Chen, Q. Li, X. Cui, L. Tang, and C. Liu, "Estimating real-time traffic carbon dioxide emissions based on intelligent transportation system technologies," *Intelligent Transportation Syst., IEEE Trans. on*, vol. 14, no. 1, pp. 469–479, 2013.

[3] M. Yilmaz and P. Krein, "Review of battery charger topologies, charging power levels, and infrastructure for plug-in electric and hybrid vehicles," *Power Electron., IEEE Trans. on*, vol. 28, no. 5, pp. 2151–2169, 2013.

[4] U. Madawala and D. Thrimawithana, "A bidirectional inductive power interface for electric vehicles in v2g syst.," *Ind. Electron., IEEE Trans. on*, vol. 58, no. 10, pp. 4789–4796, 2011.

[5] E. Sortomme and M. El-Sharkawi, "Optimal scheduling of vehicle-togrid energy and ancillary services," *Smart Grid, IEEE Trans. on*, vol. 3, no. 1, pp. 351–359, 2012.

[6] H. Hoimoja, A. Rufer, G. Dziechciaruk, and A. Vezzini, "An ultrafast ev charging station demonstrator," in *Power Electron., Electrical Drives, Automation and Motion (SPEEDAM),* 2012 International Symposium on, pp. 1390–1395, 2012.

[7] H. Akagi and H. Sato, "Control and performance of a doubly-fed induction machine intended for a flywheel energy storage system," *Power Electron., IEEE Trans. on*, vol. 17, no. 1, pp. 109–116, 2002.

[8] S. Samineni, B. Johnson, H. Hess, and J. Law, "Modeling and analysis of a flywheel energy storage system for voltage sag correction," *Industry Appl., IEEE Trans. on*, vol. 42, no. 1, pp. 42–52, 2006.

[9] Tomislav Dragicevic, Stjepan Sucic, Juan C. Vasquez, Josep M. Guerrero, "Flywheel-Based Distributed Bus Signalling Strategy for the Public Fast Charging Station", *smart grid, IEEE tran. on*, vol.PP: no.99. 1-11, 2014.

[10] Xiaonan Lu; Kai Sun; Guerrero, J.M.; Vasquez, J.C.; Lipei Huang; Teodorescu, R., "SoC-based droop method for distributed energy storage in DC microgrid applications," *Industrial Electronics (ISIE), 2012 IEEE International Symposium on* , vol., no., pp.1640,1645, 28-31 May 2012; doi: 10.1109/ISIE.2012.6237336

[11] Xiaonan Lu; Kai Sun; Guerrero, J.M.; Vasquez, J.C.; Lipei Huang, "State-of-Charge Balance Using Adaptive Droop Control for Distributed Energy Storage Systems in DC Microgrid Applications," *Industrial Electronics, IEEE Transactions on* , vol.61, no.6, pp.2804,2815, June 2014

[12] H. Kakigano, Y. Miura, and T. Ise, "Distribution voltage control for dc microgrids using fuzzy control and gain-scheduling technique," *Power Electronics, IEEE Transactions on*, vol. 28, no. 5, pp. 2246–2258, 2013.

[13] T. Dragicevic, J. Guerrero, J. Vasquez, and D. Skrlec, "Supervisory control of an adaptive-droop regulated dc microgrid with battery management capability," *Power Electronics, IEEE Transactions on*, vol. 29, no. 2, pp. 695-706, Feb. 2014.

[14] E. Twinning and D. G. Holmes, "Grid current regulation of a three-phase voltage source inverter with an LCL input filter," *Power Electron IEEE Tranaction.on*, vol. 18, no. 3, pp. 888–895, May 2003.